Stochastic self-consistent Green's function second-order perturbation theory (sGF2)

Daniel Neuhauser,[1,*] Roi Baer,[2,†] and Dominika Zgid[3,‡]

[1] *Department of Chemistry and Biochemistry, University of California at Los Angeles, California 90095 USA*
[2] *Fritz Haber Center for Molecular Dynamics, Institute of Chemistry, The Hebrew University of Jerusalem, Jerusalem 91904, Israel*[§]
[3] *Department of Chemistry, University of Michigan, Ann Arbor, Michigan 48109, USA*

The second-order Green's function method (GF2) was shown recently to be an accurate self-consistent approach for electronic structure of correlated systems since the self-energy accounts for both the weak and some of the strong correlation. The numerical scaling of GF2 is quite steep however, $O(N^5)$ (where the pre-factor is often hundreds), effectively preventing its application to large systems. Here, we develop a stochastic approach to GF2 (sGF2) where the self-energy is evaluated by a random-vector decomposition of Green's functions so that the dominant part of the calculation scales quasi linearly with system size. A study of hydrogen chains shows that the resulting approach is numerically efficient and accurate, as the stochastic errors are very small, 0.05% of the correlation energy for large systems with only a moderate computational effort. The method also yields automatically efficient MP2 energies and is automatically temperature dependent.

arXiv:1603.04141v1 [physics.chem-ph] 14 Mar 2016

Second-order Green's function (GF2) is a temperature dependent self-consistent perturbation approach where the Green's function is iteratively renormalized. Thus, at self-consistency the self-energy which accounts for the many-body correlation effects is a functional of the Green's function, $\Sigma(G)$. Upon convergence the method includes all second order skeleton diagrams dressed with the renormalized second order Green's function propagators, as illustrated in Fig. 1. Specifically, as shown in Ref. 1, GF2, which at convergence is reference independent, preserves the desirable features of Møller-Plesset perturbation theory (MP2) while avoiding the divergences that appear when static correlation is important. Additionally, GF2 possesses only a very small fractional charge and spin error,[2] less than either typical hybrid density functionals or RPA with exchange, therefore having a minimal self-interaction error. In solids[3] GF2 describes metallic, insulating, and Mott regimes and recovers the internal energy for multiple phases present in a solid. Moreover, GF2 is useful for efficient Green's function embedding techniques such as in the self-energy embedding method (SEET).[4,5]

While GF2 has these formal advantages, it is quite expensive and can be easily applied only to small systems with up to a few hundred atomic orbitals (AOs). This is because the calculation of the self-energy matrix scales as $O(n_\tau N^5)$, where n_τ is the size of the imaginary time grid and N the number of AOs. Here, we therefore develop a statistical formulation which converts the many-indices summation inherent in the self-energy matrix to a quasi linearly-scaling approach.

The present development is in the same spirit as our previous work on several electronic structure methods, including MP2,[6,7] RPA,[8] DFT,[9,10] DFT with long-range exact exchange,[11] TDDFT,[12] and GW.[13] Among these, the closest to this work are the stochastic version of MP2 in real-time plane-waves,[7] and MO-based MP2 with Gaussian basis sets.[6] The present stochastic temperature dependent MP2 and GF2 are based on a primary ingredient, the imaginary-time Green's function in an AO basis, which is attractive for stochastic simulations since it is smooth and varies continuously with parameter changes. We also note other works which use stochastic sampling of perturbative quantum chemistry expressions, including for example perturbative stochastic approaches[14] which employs different sampling schemes than ours, and a stochastic coupled clusters algorithm (CC).[15]

The correlated Green's function is

$$G(i\omega_n) = \left[[G_0(i\omega_n)]^{-1} - \Sigma(i\omega_n)\right]^{-1}, \tag{1}$$

with $G_0(i\omega_n) = \left[(\mu + i\omega_n)S - F\right]^{-1}$, where S and F are overlap and Fock matrices in the non-orthogonal AO basis and μ is the chemical potential. The Matsubara frequencies $\omega_n = (2n+1)\pi/\beta$ form a numerical grid where β is the inverse temperature and n is a non-negative integer. Recall that the relation between quantities in Matsubara frequencies and imaginary time is analogous to the relation between real-frequencies and time, i.e., $G(i\omega_n) = \int_0^\beta e^{i\omega_n\tau}G(\tau)dt$, $G(\tau) = \frac{2}{\beta}\mathrm{Re}\sum_n e^{-i\omega_n\tau}G(i\omega_n)$. Further, an important feature is that $G(\tau)$ is a smooth function of τ. For example, $G_0(\tau)$ has a form

$$G_0(\tau) = \frac{e^{-\tau(\tilde{F}-\mu 1)}}{1+e^{-\beta(\tilde{F}-\mu 1)}}, \tag{2}$$

where $\tilde{F}$ is the Fock matrix in an orthogonal basis and the resulting $G_0(\tau)$ can be transformed to a non-orthogonal AO basis if desired. Thus, $G_0(\tau)$ and $G(\tau)$ do not have the oscillations of real-time Green's functions, and this is especially important for the stochastic numerics below.

The Green's function is iteratively improved by updating the Fock-matrix F and the second order self-energy $\Sigma(i\omega_n)$ that describes the correlation effects. In GF2, the self-energy is

$$\Sigma_{ij}(\tau) = \sum_{klmnpq} G_{kl}(\tau)G_{mn}(\tau)G_{pq}(\beta-\tau)v_{ikmq} \times(2v_{ljpn} - v_{pjln}). \tag{3}$$

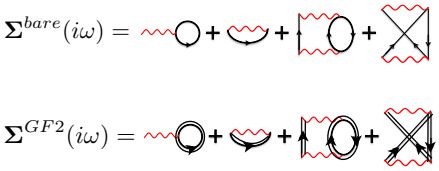

FIG. 1. Bare and dressed second-order self-energy diagrams.

The Fock matrix here is $F = h + \Sigma_\infty$ where h includes the kinetic and nuclear-electron parts and Σ_∞ is the static, frequency independent part of the self-energy $[\Sigma_\infty]_{ij} = \sum_{kl} P_{kl}(v_{ijkl} - 0.5v_{ilkj})$, evaluated from the density matrix P and the two-body integrals $v_{ijkl} = \iint d\mathbf{r}d\mathbf{r}'\phi_i(\mathbf{r})\phi_j(\mathbf{r})|\mathbf{r}-\mathbf{r}'|^{-1}\phi_k(\mathbf{r}')\phi_l(\mathbf{r}')$, assuming a real AO basis.

Typically, in the first iteration we obtain the density matrix P from a Hartree-Fock (HF) solution; however, at convergence due to the iterations GF2 is formally reference independent, so the initial Fock-matrix can be DFT-based. Beyond the first iteration, the density matrix is evaluated using the correlated Green's function as $P = \frac{2}{\beta}\sum_n e^{i\omega_n 0^+} G(i\omega_n)$ from which one constructs the Fock matrix.

Given the initial density matrix and Fock matrix, one iteratively constructs (until self-consistency is reached) self-energy matrices $\Sigma(i\omega_n)$ and Σ_∞, and the correlated Green's function, density and Fock matrices. The chemical potential μ is adjusted at each stage so that $\mathrm{Tr}(PS)$ yields the correct number of electrons, N_e.

In GF2, both the Green's function and self-energy are smooth functions of the imaginary time and frequency. At each stage, $G(i\omega_n)$ is calculated and transformed to yield $G(\tau)$, which is used to make the time-dependent self-energy $\Sigma(\tau)$ which is then transformed to give $\Sigma(i\omega_n)$. For computational efficiency, we use a non-equidistant spline grid[16] sampling the Matsubara frequencies. In the time domain, $\Sigma(\tau)$ is expressed in an orthogonal polynomial basis.[17]

The total energy is evaluated as:

$$E = \frac{1}{2}\mathrm{Tr}\left[(h+F)\,P\right] + \frac{2}{\beta}\sum_n \mathrm{Re}\big(\mathrm{Tr}[G(i\omega_n)\Sigma^T(i\omega_n)]\big), \tag{4}$$

where the latter term can be also be also evaluated as $-\int \mathrm{Tr}\big(G(\tau)\Sigma(\beta-\tau)\big)d\tau$. The GF2 correlation energy is defined as the difference between the total energy and the Hartree-Fock energy, $E_{\mathrm{corr}} = E - E_{\mathrm{HF}}$. Note that in the first iteration GF2 yields automatically the temperature-dependent MP2 energy:

$$E_{\mathrm{MP2}} = \frac{1}{\beta}\sum_n \mathrm{Re}\big(\mathrm{Tr}[G_{HF}(i\omega_n)\Sigma^T(i\omega_n)]\big). \tag{5}$$

The main numerical challenge in GF2 is the determination of the time-dependent self-energy (Eq. 3), where, heuristically, two 4-index tensors are connected through three matrices. To reduce the scaling we turn to the stochastic paradigm which replaces matrices by a random average over stochastically chosen vectors

$$G_{kl}(\tau) = \big\{\eta_k(\tau)\bar{\eta}_l(\tau)\big\}, \tag{6}$$

where the curly brackets refer to a stochastic average constructed using random vectors. Here, we construct these vectors in the most symmetric way possible, i.e., based on a square-root-like decomposition of the real-symmetric matrix $G(\tau)$:

$$\eta(\tau) = A(\tau)\sqrt{|g(\tau)|}A^T(\tau)\eta^0(\tau) \tag{7}$$

$$\bar{\eta}(\tau) = A(\tau)\frac{g(\tau)}{\sqrt{|g(\tau)|}}A^T(\tau)\eta^0(\tau), \tag{8}$$

where we introduced the eigenvectors and eigenvalues of the Green's function, $G(\tau) = A(\tau)g(\tau)A^T(\tau)$, while $\eta^0(\tau)$ is a completely random vector, i.e., $\eta^0_j(\tau) = \pm 1$ for $j = 1, ..., N$. It is straightforward to prove Eq. 6 based on the fact that $\big\{\eta^0_k(\tau)\eta^0_l(\tau)\big\} = \delta_{kl}$.

We similarly separate the other two $G(\tau)$ matrices from Eq. 3, writing them as $G_{mn}(\tau) = \big\{\zeta_m(\tau)\bar{\zeta}_n(\tau)\big\}$ and $G_{pq}(\beta-\tau) = \big\{\xi_p(\beta-\tau)\bar{\xi}_q(\beta-\tau)\big\}$. The self-energy matrix becomes then an average over a separable product:

$$\Sigma_{ij}(\tau) = \big\{\bar{u}_i(\tau)(2u_j(\tau) - w_j(\tau))\big\}, \tag{9}$$

where formally $u_i(\tau) = \sum_{kmq}\eta_k(\tau)\zeta_m(\tau)\xi_q(\beta-\tau)v_{ikmq}$ with analogous expressions for $\bar{u}, w$ (see below). It is efficient to evaluate these summations on a grid, i.e., we define a time- and space-dependent random function on a grid

$$\eta(\mathbf{r},\tau) = \sum_l \eta_l(\tau)\phi_l(\mathbf{r}), \tag{10}$$

with similar expressions for $\zeta(\mathbf{r},\tau)$, $\xi(\mathbf{r},\tau)$, etc. (The computation of these functions is linear in system size since the AO functions are local.) We then write the vectors decomposing $\Sigma(\tau)$ as convolution integrals:

$$\begin{aligned} u_j(\tau) &= (\phi_j\eta(\tau)|\zeta(\tau)\xi(\beta-\tau)) \\ &\equiv \iint \phi_i(\mathbf{r})\eta(\mathbf{r},\tau)||\mathbf{r}-\mathbf{r}'|^{-1}\zeta(\mathbf{r}',\tau)\xi(\mathbf{r}',\beta-\tau)d\mathbf{r}d\mathbf{r}', \end{aligned} \tag{11}$$

and analogously $w_j(\tau) = (\phi_j\xi(\beta-\tau)|\zeta(\tau)\eta(\tau))$, $\bar{u}_j(\tau) = (\phi_j\bar{\eta}(\tau)|\bar{\zeta}(\tau)\bar{\xi}(\beta-\tau))$. Therefore, the expensive summation over many indices is replaced by averaging over convolution integrals, each of which scales quasi-linearly with system size.

In passing, we note that the formalism is completely robust to near-degeneracies in the basis due to the transformations in Eqs. 7,8. This is in contrast to other formally simpler stochastic evaluations of the self-energy, e.g., choosing randomly all the non$-ij$ indices in Eq.3.

Computational details. To study the performance of stochastic GF2 we used typical model systems, finite (non-periodic) chains of hydrogen atoms spaced 1 Å apart with N =30, 100, 300 and 1000. A minimal STO-3G basis set was used so $N = N_e$. A numerical grid contained up to 10×10×4000 points with a 0.5 bohr spacing was sufficient for converging Eq. 11. The convolution integrals employed the usual numerical-analytical splitting[18] which uses here grid-doubled integration due to the lack of periodicity in any dimension. The inverse temperature was set at $\beta = 50$ 1/a.u. and a Chebyshev-type imaginary-time grid[17] with 128 time points was employed. As mentioned, a spline-fit method was used[16] for the frequency-to-time conversions of $G(i\omega_n)$ and $\Sigma(i\omega_n)$ and for the evaluation of the two-body energy.

The completely-random vectors (η^0,ζ^0,ξ^0) were different at each time point τ but did not change with the self-consistent GF2 iterations. A key for the self-consistency convergence was DIIS (direct inversion of the iterative subspace).[19,20] After each iteration a combined vector made from the τ-dependent self-energy $\Sigma(\tau)$ and the Fock matrix (weighted by a factor, typically 3.0) was fed into a general DIIS routine that held in memory the 4 previous iterations and updated the combined vector. The simulations started with Hartree-Fock densities, and about 12 iterations were required for the DIIS convergence to an error which was much smaller than the statistical (sampling) error. The number of stochastic samples, N_{MC}, ranged between 50 and 800, and the results were averaged over several simulations starting from different random numbers.

Temperature-dependent MP2. The first SGF2 iteration yields the MP2 correlation energy (Eq. 5) which follows a Gaussian distribution as illustrated in Fig. 2. Table I shows the correlation energy $E_{\rm corr}$ and the (stochastic) error $\delta E_{\rm corr}$ for chains with various number of orbitals. Even for $N = 1000$, the stochastic error is only 0.058% of the total correlation energy. For perspective, note that (deterministic) errors of larger or similar magnitude are present in local or divide and conquer MP2 methods with density fitting[21,22].

Stochastic GF2. In sGF2, due to the iterations, the dependence of the energy on the Green function, which depends itself on the number (N_{MC}) of stochastic sampling of Eq.9, leads to an additional non-stochastic (bias) dependence on N_{MC}. (Simply put, averaging a million sGF2 calculations each with 100 stochastic samples will give different results than averaging 100 simulations which each uses a million samples, unlike in sMP2.) Mathematically, the energy in any specific simulation with N_{MC} samplings is then approximately $E = E(N_{MC}) + r(N_{MC})^{-\frac{1}{2}}\delta$, where $E(N_{MC})$ is a bias-type component, r is a random scale-less variable, and δ is approximately independent of N_{MC}. Specifically, as seen in Figs. 3 and 4, the energies for different N_{MC} are stochastically distributed around a line $E(N_{MC})$. We found excellent fit to an empirical formula

$$E(N_{MC}) - E_{\rm HF} = E_{\rm corr} + b(N_{MC})^{-\frac{4}{3}} \qquad (12)$$

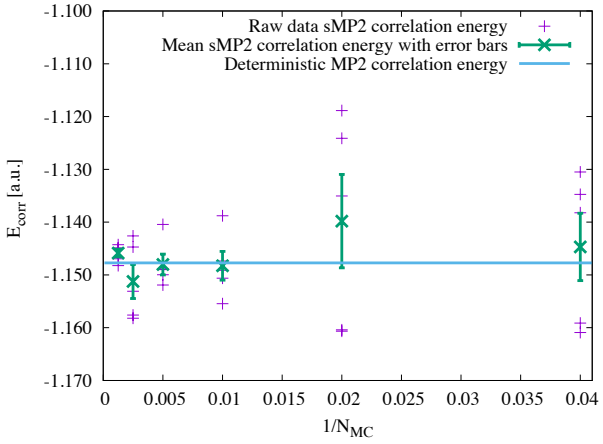

FIG. 2. The stochastic and deterministic thermal MP2 correlation energies for different N_{MC} for hydrogen chain with N=100.

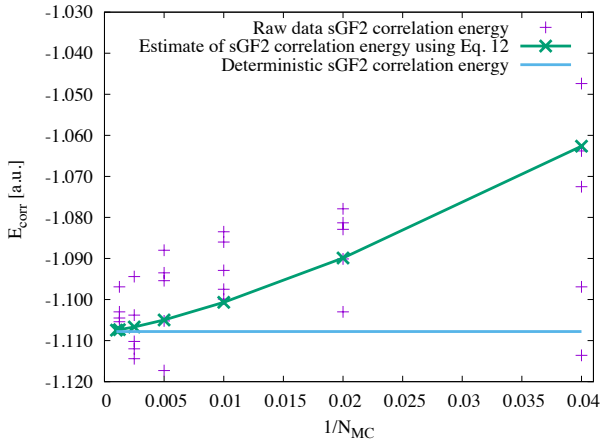

FIG. 3. The stochastic and deterministic GF2 correlation energies for different N_{MC} for hydrogen chain with N=100.

i.e., the stochastic calculated energies cluster near the line defined by this formula. We therefore fit, for any given system, the values of b, and $E_{\rm corr}$ that yield the best fit to the actual calculated data. The fitted value of $E_{\rm corr}$ is the GF2 prediction for the correlation energy. Note that an alternative is to reduce the dependence of the curve (i.e., to flatten the $E(N_{MC})$ bias-dependence on N_{MC}) by employing in Eq. 4 Green's functions and self-energies that come from different sets of stochastic runs, in the spirit of "jackknife" analysis[23].

The sGF2 results, summarized in Table I, show that the self-consistent iterations that are inherent in GF2 do not destroy the convergence of the method. Further, in large systems the GF2 correlation reduces the spatial extent of Σ_∞ so the statistical error even decreases relative to sMP2. The statistical error in the total energy would have grown as $\sqrt{N}$ if the system was made from completely isolated non-interacting fragments, and the results here overall follow this trend.

Timings. Overall the calculations took, for the largest

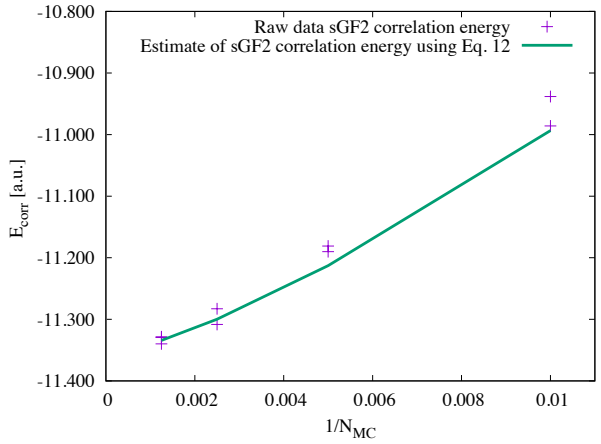

FIG. 4. The stochastic GF2 correlation energies for different N_{MC} for hydrogen chain with N=1000.

Method	N	$E_{\rm corr}$	$\delta E_{\rm corr}$	b
sGF2	30	-0.307	0.0013	-0.9
	100	-1.104	0.0021	3.3
	300	-3.388	0.0032	12.0
	1000	-11.357	0.0057	168.7
sMP2	30	-0.337	0.0009	
	100	-1.148	0.0016	
	300	-3.472	0.0027	
	1000	-11.610	0.0067	

TABLE I. Stochastic GF2 and MP2 correlation energies in Hartree using 4000 total Monte Carlo runs (composed of several sets of runs with different values of N_{MC}) for different number of orbitals in hydrogen chains. For each system, an empirical formula $E - E_{HF} = E_{\rm corr} + b\,(N_{MC})^{-\frac{4}{3}}$ was fitted to the calculated energies, so $E_{\rm corr}$ is the predicted GF2 correlation energy.

system size ($N_e = 1000$), 6500 core hours on standard 2Gflops CPUs, and the method is fully parallelized. The temperature-dependent MP2 evaluations only require the first (of twelve) SCF iterations so they took only 500 CPU core hours for the largest system. The calculation times are dominated by the stochastic evaluation of the self-energy which rises linearly with system size. For finite systems beyond ≈ 5000 orbitals the quadraticly and cubicly rising parts in the non-stochastic GF2 parts (e.g., inversion and diagonalization of the Green's functions, etc.) would start dominating the scaling.

In conclusion, we presented an sGF2 algorithm and evaluated electronic correlation energies for prototypical hydrogen chain systems. We demonstrated that the stochastic GF2 errors are well controlled and highly accurate correlation energies with only a 0.05% stochastic error are reached with reasonable computational effort. These errors are comparable with errors of local MP2 approaches used in quantum chemistry. The present calculations are among the first applications of fully self-consistent Green's function method with full imaginary frequency dependence to large systems described by a full quantum chemistry Hamiltonian. Moreover, we demonstrated that the splitting of matrices by a random average over stochastically chosen vectors leads to a small variance and that relatively few Monte Carlo samples already yield quite accurate correlation energies. The reason for this is two-fold: the stochastic sampling inherently acts only in the space of orbitals but the actual spatial integrals (Eq. 11) are evaluated exactly; in addition, since the Green's function matrices are smooth in imaginary time, different random vectors can be used at each imaginary-time point thereby enhancing the stochastic sampling efficiency.

There are many possible applications and extensions of the approach studied here. sGF2 is potentially suitable for calculating energy differences between neighboring configurations because the underlying stochastic vectors are chosen automatically in the AO space so they are continuous with a change of the system parameters; this is in contrast with our previous stochastic MP2 basis in Gaussian basis study[6] where the stochastic vectors were chosen in the MO space so they were not continuous with change of parameters.

Further, the present stochastic GF2 and MP2 methods are automatically suitable for periodic systems, as all the deterministic steps (i.e., Eq. 1) and the time-frequency transforms are very efficient when done in the reciprocal (k) space. The only caveat is that in periodic systems one needs to choose the random vectors to be in k-space and then to convert them to real-space, as detailed in an upcoming article.

Finally, we also note that, beyond the results presented here, it should also be possible to achieve further reduction of the stochastic error with an embedded fragment approach similar to self-energy embedding approaches where a deterministic self-energy is embedded into the stochastic estimate of self-energy for a larger fragment.

Discussions with Eran Rabani are gratefully acknowledged. D.N. and D.Z. were supported by the NSF, grants CHE-1112500 and CHE-1453894, respectively. D.N. and R.B. were also supported by the BSF grant 2012050. R.B. is supported by the Israel Science Foundation–FIRST Program (Grant No. 1700/14), and is supported for his sabbatical visit by the Pitzer Center and the Kavli Institute of the University of California, Berkeley.

* dxn@ucla.edu
† roi.baer@huji.ac.il
‡ zgid@umich.edu
§ Roi Baer is on Sabbatical leave in the Department of

Chemistry, University of California, Berkeley, California 94720, USA

[1] J. J. Phillips and D. Zgid, *J. Chem. Phys.* **140**, 241101 (2014).

[2] J. J. Phillips, A. A. Kananenka, and D. Zgid, *The Journal of Chemical Physics* **142**, 194108 (2015).

[3] A. A. Rusakov and D. Zgid, *The Journal of Chemical Physics* **144**, 0541102 (2016).

[4] A. A. Kananenka, E. Gull, and D. Zgid, *Phys. Rev. B* **91**, 121111 (2015).

[5] T. N. Lan, A. A. Kananenka, and D. Zgid, *The Journal of Chemical Physics* **143**, 241102 (2015).

[6] D. Neuhauser, E. Rabani, and R. Baer, *Journal of Chemical Theory and Computation* **9**, 24 (2013).

[7] Q. Ge, Y. Gao, R. Baer, E. Rabani, and D. Neuhauser, *The Journal of Physical Chemistry Letters* **5**, 185 (2014).

[8] D. Neuhauser, E. Rabani, and R. Baer, *The Journal of Physical Chemistry Letters* **4**, 1172 (2013).

[9] Y. Cytter, D. Neuhauser, and R. Baer, *Journal of Chemical Theory and Computation* **10**, 4317 (2014).

[10] D. Neuhauser, R. Baer, and E. Rabani, *The Journal of Chemical Physics* **141**, 041102 (2014).

[11] R. Baer and D. Neuhauser, *The Journal of Chemical Physics* **137**, 051103 (2012).

[12] Y. Gao, D. Neuhauser, R. Baer, and E. Rabani, *The Journal of Chemical Physics* **142**, 034106 (2015).

[13] D. Neuhauser, Y. Gao, C. Arntsen, C. Karshenas, E. Rabani, and R. Baer, *Phys. Rev. Lett.* **113**, 076402 (2014).

[14] S. Y. Willow, J. Zhang, E. F. Valeev, and S. Hirata, *The Journal of Chemical Physics* **140**, 031101 (2014).

[15] A. J. W. Thom, *Phys. Rev. Lett.* **105**, 263004 (2010).

[16] A. A. Kananenka, A. R. Welden, T. N. Lan, E. Gull, and D. Zgid, *arXiv:1602.05898* .

[17] A. A. Kananenka, J. J. Phillips, and D. Zgid, *Journal of Chemical Theory and Computation* **12**, 564 (2016).

[18] G. J. Martyna and M. E. Tuckerman, *The Journal of Chemical Physics* **110**, 2810 (1999).

[19] P. Pulay, *Chemical Physics Letters* **73**, 393 (1980).

[20] P. Pulay, *Journal of Computational Chemistry* **3**, 556 (1982).

[21] H.-J. Werner, F. R. Manby, and P. J. Knowles, *The Journal of Chemical Physics* **118**, 8149 (2003).

[22] P. Baudin, P. Ettenhuber, S. Reine, K. Kristensen, and T. Kjærgaard, *The Journal of Chemical Physics* **144**, 054102 (2016).

[23] M. Troyer, *Computational Physics*, ETH Zurich, 2005.